# Fermi Resonance Involving Nonlinear Dynamical Couplings in Pb(Zr, Ti)$O_3$ Solid Solutions

Dawei Wang,[1,2,*] Elena Buixaderas,[3] Jorge Íñiguez,[4] Jeevaka Weerasinghe,[2] Hong Wang,[5] and L. Bellaiche[2]

[1]*Shaanxi Key Laboratory of Photonics Technology for Information and Key Laboratory for Physical Electronics and Devices of the Ministry of Education, School of Electronic and Information Engineering, Xi'an Jiaotong University, Xi'an 710049, China**

[2]*Physics Department, University of Arkansas, Fayetteville, Arkansas 72701, USA*

[3]*Institute of Physics, Academy of Sciences of the Czech Republic, Na Slovance 2, 18221 Prague 8, Czech Republic*

[4]*Institut de Ciència de Materials de Barcelona (ICMAB-CSIC), Campus UAB, 08193 Bellaterra, Spain*

[5]*School of Electronic and Information Engineering, Xi'an Jiaotong University, Xi'an 710049, China*

(Received 19 June 2011; published 17 October 2011)

We have used first-principles-based simulations and Raman scattering techniques to reveal a novel dynamical phenomenon in Pb(Zr, Ti)$O_3$ solid solutions: a Fermi resonance (FR) emerging from the nonlinear coupling between ferroelectric (FE) motions and tiltings of oxygen octahedra. This FR manifests itself as the doubling of a nominally single FE mode in a purely FE phase, when the resonant frequency of the FE mode is close to the first overtone of the tiltings. We show that the FR is the result of a nonlinear coupling that is proportional to the spontaneous polarization of the material and derive an analytical model that captures the essence of the effect.

DOI: 10.1103/PhysRevLett.107.175502 PACS numbers: 77.84.Cg, 63.20.K−, 63.20.Ry, 77.80.−e

Ferroelectrics (FE) form an important class of materials that has been used in many devices [1]. Several crucial properties of FE materials are solely due to electrical dipoles. These dipoles, however, are not the only degree of freedom in various FE compounds. For instance, antiferrodistortive (AFD) motions, which correspond to the tilting of oxygen octahedra, also exist in the technologically important Pb(Zr, Ti)$O_3$ (PZT) solid solution [2–6]. Similarly, one of the most currently studied class of materials, namely, multiferroics, also possesses magnetic dipoles [7]. Interestingly, the *coupling* between the electric dipoles and the other degree(s) of freedom can lead to novel effects of fundamental and technological interest. For instance, an additional peak of $E$ symmetry emerges at low temperature in PZT systems because of FE and AFD interactions [4,5,8,9]. Another example is electromagnons that manifest themselves as additional dielectric (or Raman) peaks in the GHz-THz regime in multiferroics [10–12]. These peaks occur only if the crystallographic phase is ''doubly'' ordered, e.g., if it possesses both a spontaneous polarization and long-range-ordered AFD or magnetic arrangement [13,14]. One may wonder if novel dielectric or Raman peaks can also occur in ferroelectrics in case of a ''singly'' ordered phase, e.g., if this phase only possesses a spontaneous polarization while the AFD motions do not adopt a long-range order (although existing locally). Determining the precise microscopic origin of such hypothetical novel peaks (if any) is also of obvious importance.

Here, we report that such a phenomenon indeed exists in ferroelectrics, via the combination of computational, theoretical, and experimental techniques: two peaks of $A_1$ symmetry are found in PZT in the purely FE phase, when the resonant frequency of the $A_1$ mode is close to the resonant frequency of the first overtone of the AFD motions. Such previously overlooked doubling is a manifestation of Fermi resonance [15] involving nonlinear couplings between FE ad AFD motions.

We investigate the $Pb(Zr_{0.47}Ti_{0.53})O_3$ solid solution by using the effective Hamiltonian approach of Ref. [6]. In addition to homogeneous and inhomogeneous strains, this scheme has 2 degrees of freedom in each unit cell $i$: (1) the local soft-mode displacement, $\boldsymbol{u}_i$ (the product of $\boldsymbol{u}_i$ with a Born effective charge $Z^*$ is the electric dipole centered on the unit cell $i$); and (2) $\boldsymbol{\omega}_i$ that characterizes AFD motion in the unit cell $i$. The direction of $\boldsymbol{\omega}_i$ is the axis about which the oxygen octahedron tilts while its magnitude provides the angle of such tilting [6]. The total energy of the effective Hamiltonian approach consists of a sum of three terms, $E_{\text{tot}} = E_{\text{FE}}(\{\boldsymbol{u}_i\}, \{\boldsymbol{v}_i\}, \eta_H, \{\sigma_j\}) + E_{\text{AFD}}(\{\boldsymbol{\omega}_i\}, \{\boldsymbol{v}_i\}, \eta_H, \{\sigma_i\}) + E_{\text{coupl}}(\{\boldsymbol{u}_i\}, \{\boldsymbol{\omega}_i\})$, where $\{\boldsymbol{v}_i\}$ are related to the inhomogeneous strain variables inside each cell, $\eta_H$ is the homogeneous strain tensor, and $\{\sigma_i\}$ characterizes the atomic arrangement; that is, $\sigma_i = +1$ $(-1)$ represents a Zr (Ti) atom sitting at the site $i$. $E_{\text{FE}}$ and $E_{\text{AFD}}$ gather the energetic terms solely involving the $\boldsymbol{u}_i$ and $\boldsymbol{\omega}_i$ degrees of freedom, respectively. $E_{\text{coupl}}$ characterizes the interactions between FE and AFD motions and is given by

$$E_{\text{coupl}}(\{\boldsymbol{u}_i\}, \{\boldsymbol{\omega}_i\}) = \sum_{i,\alpha,\beta,\gamma,\delta} D_{\alpha\beta\gamma\delta}\omega_{i,\alpha}\omega_{i,\beta}u_{i,\gamma}u_{i,\delta}, \quad (1)$$

where $i$ runs over the unit cells and $\alpha$, $\beta$, $\gamma$, and $\delta$ denote Cartesian components—with the $x$, $y$, and $z$ axes being chosen along the pseudocubic [100], [010], and [001] directions, respectively. The $D_{\alpha\beta\gamma\delta}$ coefficients quantify the couplings between the FE and AFD motions. For symmetry reasons, only three different kinds of $D_{\alpha\beta\gamma\delta}$ elements are nonzero and different from each other,

 

namely, $D_{xxxx} = D_{yyyy} = D_{zzzz}$, $D_{xxyy} = D_{yyxx} = D_{yyzz} = D_{zzyy} = D_{zzxx} = D_{xxzz}$, and $D_{xyxy} = D_{yxyx} = D_{yzyz} = D_{zyzy} = D_{zxzx} = D_{xzxz}$. These three kinds of coefficients are hereafter denoted by $D_1$, $D_2$, and $D_3$, respectively.

We use $12 \times 12 \times 12$ supercells (8640 atoms) in which Zr and Ti atoms are randomly distributed to mimic disordered solid solutions. The effective Hamiltonian is then put into molecular dynamics simulations to obtain finite-temperature properties. For the chosen Ti composition of 53%, a cubic paraelectric phase is found for temperatures above ~800 K and a $P4mm$ tetragonal phase in which the polarization points along a $\langle 001 \rangle$ direction exists between the Curie temperature $T_C \sim 800$ K and another critical temperature ~120 K. Such predictions agree well with experiments [2,3,16]. As in Ref. [6], a $I4cm$ state is predicted to occur below ~120 K. In this state, the oxygen octahedra tilt, in a long-range fashion, about the same $\langle 001 \rangle$ polarization direction (with neighboring oxygen octahedra rotating in antiphase)—which is consistent with some recent measurements [6,17]. The numerical scheme of Refs. [9,18] is used to extract complex dielectric responses at different temperatures, and each peak found in the dielectric spectra is fitted by a classical harmonic oscillator $\varepsilon(\nu) = S\nu_r^2/(\nu_r^2 - \nu^2 + i\nu\gamma_r)$, where $\nu_r$, $\gamma_r$, and $S$ are the resonant frequency, damping constant, and oscillator strength of the oscillator, respectively.

Figures 1(a) and 1(b) display the real and imaginary parts of the isotropic dielectric response—i.e., $[\varepsilon_{xx}(\nu) + \varepsilon_{yy}(\nu) + \varepsilon_{zz}(\nu)]/3$—of the studied PZT system versus frequency at 600 and 400 K, respectively. The insets of such figures show the $\varepsilon_{zz}(\nu)$ dielectric response, where $z$ corresponds to the polarization's direction. Figure 1(a) indicates that PZT behaves "normally" at 600 K; i.e., it possesses a doubly degenerate $E$ mode at lower frequencies and a single $A_1$ mode at higher frequencies. Note that

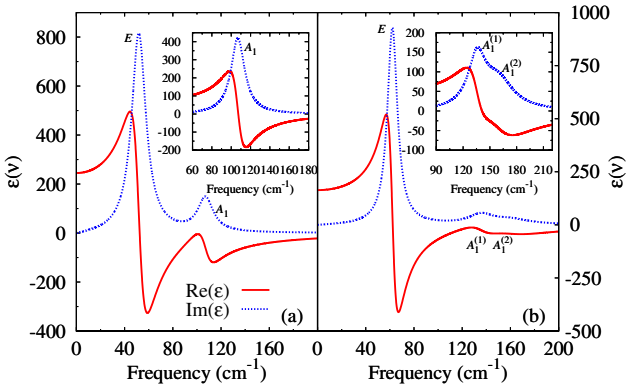


FIG. 1 (color online). The isotropic dielectric response of the $Pb(Zr_{0.47}Ti_{0.53})O_3$ solid solution versus frequency, at (a) 600 K and (b) 400 K. The insets show the $\varepsilon_{zz}$ dielectric response, where $z$ corresponds to the direction of the polarization. Solid and dotted lines represent the real and imaginary parts, respectively, of such complex dielectric responses.

the $E$ (respectively, $A_1$) mode corresponds to atomic vibrations perpendicular (respectively, parallel) to the direction of the spontaneous polarization. One important feature revealed by Fig. 1(b) is the "abnormal" existence of two $A_1$ modes at 400 K. These two modes are denoted as $A_1^{(1)}$ and $A_1^{(2)}$ in the following, and their resonant frequencies are around 136 and 161 $cm^{-1}$, respectively, at 400 K. It is important to realize that the crystallographic phase is identical between 400 and 600 K (that is, $P4mm$). In other words, the doubling of the $A_1$ modes is not associated with a phase transition, unlike the extra $E$ mode that occurs at low temperature [9,13]. Further simulations for PZT systems with different compositions in the morphotropic phase boundary, as well as using different supercell sizes, were also performed at 300 and 400 K, and two $A_1$ modes were also found there. This doubling of the $A_1$ mode thus appears to be a general feature of PZT systems near their morphotropic phase boundary. We also conducted additional simulations in which we switched off the alloying effects in PZT; that is, we treated the studied solid solution as a simple $Pb\langle B \rangle O_3$ crystal for which $\langle B \rangle$ represents a virtual atom that is intermediate between Ti and Zr atoms [19]. In that simplified case, the doubling of the $A_1$ mode is still present at 300 K, which implies that such a doubling has nothing to do with the presence of two B atoms in PZT (Ti and Zr).

Interestingly, one Raman experiment [20] previously reported an active mode with a frequency of $\simeq 125$ $cm^{-1}$, while another infrared measurement indicated a resonant frequency around 160 $cm^{-1}$ at room temperature in a $Pb(Zr_{0.55}Ti_{0.45})O_3$ solid solution [21]. The fact that these two experimental frequencies are very close to our predictions strongly hints towards the possibility that one measurement determined the frequency of what we denoted as the $A_1^{(1)}$ mode while the other measurement "saw" the $A_1^{(2)}$ mode—with none of these two experiments realizing that two modes with $A_1$ symmetry can exist in PZT at room temperature within the $\simeq$ 100–170 $cm^{-1}$ range [22].

To better understand this unusual doubling of the $A_1$ mode, Fig. 2 shows the temperature dependence of the resonant frequencies for the $A_1$ peaks found in our simulations for $Pb(Zr_{0.47}Ti_{0.53})O_3$. Just below $T_C$ and down to 525 K, only a single $A_1$ mode exists. The frequency of this mode follows there a square-root law, i.e., $\nu_r \sim |T_C - T|^{1/2}$. On the other hand, for temperatures ranging between ~500 K and ~100 K, two modes of $A_1$ symmetry exist, with the $A_1^{(1)}$ (respectively, $A_1^{(2)}$) mode having a frequency lower (respectively, higher) than that given by the square-root law. Furthermore, for temperatures below ~100 K, the $A_1^{(1)}$ and $A_1^{(2)}$ modes merge into a single mode of $A_1$ symmetry that follows again the square-root law. Figure 2 further reveals that the highest temperature at which the single $A_1$ mode disappears in favor of the $A_1^{(1)}$ and $A_1^{(2)}$ modes is such that the frequency of this single $A_1$ mode is

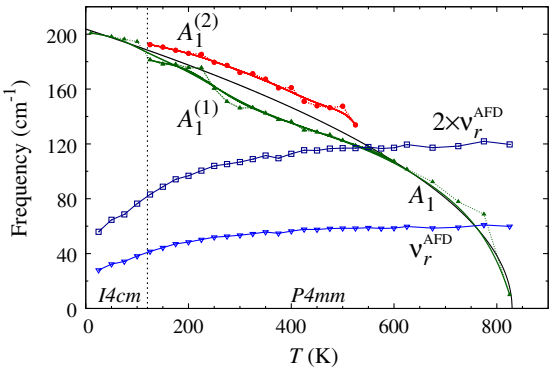


FIG. 2 (color online). Temperature dependence of the resonant frequency of the $A_1$ modes and of twice the resonant frequency of the AFD mode in $Pb(Zr_{0.47}Ti_{0.53})O_3$. The thin black solid line (without symbol) represents the fitting of the single $A_1$ mode, for temperatures above 525 K and its interpolation down to 0 K by a square-root law (i.e., $\nu_r \sim |T_c - T|^{1/2}$). The crystallographic ferroelectric phases of the system at different temperatures are also indicated.

nearly equal to twice the main resonant frequency associated with the antiphase AFD motions [23] (that are associated with the $R$ point of the first Brillouin zone [9], i.e., with a zone-boundary phonon extending in the entire crystal). Such a feature is further confirmed by additional calculations in which the resonant frequency of the AFD motions is varied by hand and strongly suggests that the coupling between the AFD and the soft modes is responsible for the doubling of the $A_1$ mode. This latter possibility is consistent with the results of additional simulations in which we turned off the AFD motions or switch off the $D_{\alpha\beta\gamma\delta}$ parameters of Eq. (1): in such cases, only a single $A_1$ mode can be seen in the dielectric spectra down to the lowest temperature. We also numerically found that the $D_2$ parameter has a stronger effect than the $D_1$ coefficient on the doubling of the $A_1$ modes, while the $D_3$ parameter has merely no effect on such doubling. It thus appears that the doubling of the $A_1$ modes mostly originates from an interaction between longitudinal FE displacement and transverse AFD motions.

The fact that the unusual $A_1$ mode doubling requires an overtone of the AFD mode to be close to the resonant frequency of the single $A_1$ mode points towards a Fermi resonance (FR) associated with nonlinear couplings [15]. Such a phenomenon is well-known in molecules [24,25] but much less documented in inorganic crystals, especially in perovskites [26–28]. Note that, if the overtone of the AFD mode becomes too far away in frequency from the "bare" single $A_1$ mode (that can be assumed to coincide with the fitted, square-root solid line of Fig. 2), then the FR cannot occur anymore. This explains the disappearance of the $A_1^{(1)}$ and $A_1^{(2)}$ modes in favor of a single $A_1$ mode for temperatures below ~100 K, as seen in Fig. 2.

In order to confirm and further understand the proposed FR, let us consider a structural phase that possesses a spontaneous polarization but in which the AFD $\boldsymbol{\omega}_i$'s do not organize themselves into a long-range order—exactly as in $P4mm$ [29]. To simplify the investigation of the dynamics of $\boldsymbol{u}_i$ and $\boldsymbol{\omega}_i$ due to their nonlinear couplings, we introduce $\tilde{\boldsymbol{u}}_i$ and $\tilde{\boldsymbol{\omega}}_i$ such as

$$\boldsymbol{u}_i(t) = \langle \boldsymbol{u} \rangle + \tilde{\boldsymbol{u}}_i(t), \qquad \boldsymbol{\omega}_i(t) = \langle \boldsymbol{\omega} \rangle + \tilde{\boldsymbol{\omega}}_i(t) = \tilde{\boldsymbol{\omega}}_i(t). \quad (2)$$

In the above equation, $t$ represents time and $\tilde{\boldsymbol{u}}_i$ (respectively, $\tilde{\boldsymbol{\omega}}_i$) is the deviation of the local mode (respectively, AFD mode) in the unit cell $i$ with respect to its spontaneous value $\langle \boldsymbol{u} \rangle$ (respectively, $\langle \boldsymbol{\omega} \rangle = 0$). Plugging Eq. (2) into Eq. (1), one finds that the essential FE-AFD nonlinear coupling term that governs the dynamics of $\tilde{\boldsymbol{u}}_i$ and $\tilde{\boldsymbol{\omega}}_i$ has the following form (see Supplemental Material [30]):

$$H_{\text{coupl,dynam}} = \sum_i \kappa \langle u \rangle \tilde{u}_i (\tilde{\omega}_i)^2, \quad (3)$$

where $\tilde{u}_i$ corresponds to the (small, dynamical, and long-range correlated) motion along the polarization direction and $\tilde{\omega}_i$ corresponds to (small, dynamical, and long-range correlated) AFD motions either perpendicularly to the polarization direction (in that case, the $\kappa$ parameter is related to the $D_2$ parameter) or parallel to that direction (in that case, $\kappa$ is proportional to $D_1$). The dynamical equation for $\tilde{u}_i$ is thus

$$\frac{d^2\tilde{u}_i}{dt^2} = -4\pi^2(\nu_r^{\text{FE}})^2\tilde{u}_i - \frac{\kappa\langle u \rangle}{m_u}(\tilde{\omega}_i)^2 + \frac{Z^* E(t)}{m_u}, \quad (4)$$

where $\nu_r^{\text{FE}}$ is the frequency of the soft mode related to the derivatives of the aforementioned $E_{\text{FE}}$ energy term and $m_u$ is the soft-mode effective mass. $E(t)$ is an applied ac electric field. Equation (4) further proves the existence of a coupling between the dynamical small (long-range correlated) displacement of the *square* of the AFD motion and the dynamical small (long-range correlated) displacement of the soft mode in a polar phase, which is consistent with the proposed occurrence of FR involving an AFD overtone. One can prove (see Supplemental Material [30]) that, when $\nu_r^{\text{FE}}$ is close to twice the AFD resonance frequency, Eq. (4) leads to two resonant frequencies for the $A_1$ mode that are given by $\nu_r^2 = \nu_{\text{FE}}^2 \pm \Omega^2$, where $\Omega^2$ depends on the $\kappa$ coupling parameter, as well as on the value of the spontaneous polarization. As Eq. (4) and $\nu_r^2$ bear similarities to the analogous expressions for typical FR (see, e.g., Ref. [31] and references therein), our simulations indeed predict that, as a consequence of the coupled dynamics of the FE and AFD modes, a Fermi resonance occurs in PZT and manifests itself as the doubling of the $A_1$ mode.

To experimentally confirm the predicted nonlinear FR, we conducted Raman measurements on $Pb(Zr_{0.48}Ti_{0.52})O_3$ ceramics [32]. The sample was prepared by a conventional mixed oxide routine using standard laboratory reagent-grade starting powders (> 99.9% purity). The density of the sample was greater than 95% of its theoretical value.

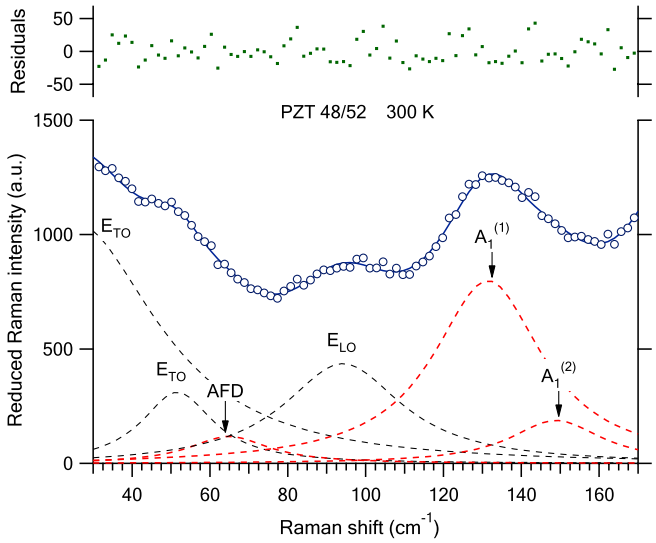


FIG. 3 (color online). Room-temperature Raman spectra of $Pb(Zr_{0.48}Ti_{0.52})O_3$ (corrected by the thermal population factor). The open symbols are the data, while the solid line represents their fit by the different peaks indicated (via dashed lines) at the bottom of the figure. Mode symmetries resulting from the effective medium approach detailed in Refs. [17,36] are indicated above each peak. The residual difference between the data and the fit is indicated on the top of the figure and is rather small—therefore emphasizing the need of having several harmonic oscillators to describe well the spectra. The dashed red lines (indicated by arrows) represent the peaks associated with AFD, $A_1^{(1)}$, and $A_1^{(2)}$ modes.

More details can be found in Ref. [16]. The Raman spectrum was obtained by exciting the optically polished sample with the 514.5 nm line from an Ar laser at a power of 25 mW. The diameter of the laser spot on the sample surface amounted to 2–3 $\mu$m, and the power on the sample was about 5 mW. The spectral resolution was better than 2 $cm^{-1}$. Raman spectra were recorded in a back-scattering geometry by a RM-1000 RENISHAW Raman spectrometer, equipped with a NExT filter to achieve the lowest frequency of 20 $cm^{-1}$. The natural polarization of the laser was used, which yields almost parallel polarization. The spectra, corrected from the instrumental function and from Bose-Einstein factor correction [33], were fitted with a sum of independent damped harmonic oscillators (modified Lorentzian shapes) using a homemade computer program. The spectrum at room temperature is shown in Fig. 3. As consistent with our simulations and other Raman experiments [34,35], such a spectrum reveals that (1) two modes are indeed necessary to fit well the data in the 120–180 $cm^{-1}$ range and (2) the resonant frequency of these two modes is close to twice the frequency of the AFD motions. The temperature dependence of these two experimental mode frequencies is also obtained (see Fig. 1 of the Supplemental Material [31]) and compares well with the simulation results depicted in Fig. 2.

In summary, computational, analytical, and experimental tools have been used to report and understand the first FR involving the soft mode and an overtone of AFD motions in any FE—as a result of nonlinear dynamical couplings. We thus hope that the present Letter enhances the current knowledge of ferroelectrics, dynamics, and nonlinear effects.

We thank J. Petzelt and J. Hlinka for insightful discussions and B. Noheda for providing the PZT sample. This work is mostly supported by the DOE, Office of Basic Energy Sciences, under Contract No. ER-46612. We also acknowledge support from the National Natural Science Foundation of China under Grant No. 10904122 (D. W.); the Czech Ministry of Education Project No. MSMT ME08109 (E. B.); MICINN Spain under Grants No. MAT2010-18113, No. MAT2010-10093-E, and No. CSD2007-00041 (J. I.); ONR Grants No. N00014-08-1-0915 and No. N00014-11-1-0384, and NSF Grants No. DMR-0701558 and No. DMR-1066158 (L. B.). Some computations were made possible thanks to the MRI Grant No. 0722625 from the NSF.

*dawei.wang@mail.xjtu.edu.cn

[1] K. Uchino, *Piezoelectric Actuators and Ultrasonic Motors*, Electronic Materials: Science & Technology (Springer, New York, 1996), 1st ed.
[2] B. Jaffe, W. Cook, and H. Jaffe, *Piezoelectric Ceramics* (Academic, London, 1971).
[3] B. Noheda, L. Wu, and Y. Zhu, Phys. Rev. B **66**, 060103 (2002).
[4] D. Bäuerle and A. Pinczuk, Solid State Commun. **19**, 1169 (1976).
[5] M. Deluca *et al.*, J. Raman Spectrosc. **42**, 488 (2011).
[6] I. A. Kornev *et al.*, Phys. Rev. Lett. **97**, 157601 (2006).
[7] G. A. SmolenskiÄ and I. E. Chupis, Sov. Phys. Usp. **25**, 475 (1982).
[8] E. Buixaderas and S. Kamba, J. Phys. Condens. Matter **13**, 2823 (2001).
[9] D. Wang, J. Weerasinghe, L. Bellaiche, and J. Hlinka, Phys. Rev. B **83**, 020301(R) (2011).
[10] A. B. Sushkov *et al.*, J. Phys. Condens. Matter **20**, 434210 (2008).
[11] A. Pimenov, A. M. Shuvaev, A. A. Mukhin, and A. Loidl, J. Phys. Condens. Matter **20**, 434209 (2008).
[12] A. Pimenov *et al.*, Phys. Rev. Lett. **102**, 107203 (2009).
[13] P. A. Fleury, J. F. Scott, and J. M. Worlock, Phys. Rev. Lett. **21**, 16 (1968).
[14] J. Petzelt and V. Dvorak, J. Phys. C **9**, 1571 (1976).
[15] E. Fermi, Z. Phys. **71**, 250 (1931).
[16] B. Noheda *et al.*, Phys. Rev. B **63**, 014103 (2000).
[17] E. Buixaderas *et al.*, Phase Transit. **83**, 917 (2010).
[18] I. Ponomareva *et al.*, Phys. Rev. B **77**, 012102 (2008).
[19] L. Bellaiche and D. Vanderbilt, Phys. Rev. B **61**, 7877 (2000).
[20] J. Meng, R. Katiyar, G. Zou, and X. Wang, Phys. Status Solidi (a) **164**, 851 (1997).

[21] V. Sivasubramanian, V. Murthy, B. Viswanathan, and M. Sieskind, J. Phys. Condens. Matter **8**, 2447 (1996).

[22] Such overlooking of these two modes likely arises from the broadness and thus overlap of the $A_1^{(1)}$ and $A_1^{(2)}$ modes in the Raman spectra. In this frequency range, there is also an $E$(LO) mode at $\sim$100 cm$^{-1}$ (depending on temperature), which creates some confusion in the symmetry assignment of Raman peaks.

[23] In fact, we found that there is another AFD resonant frequency, in addition to the main one shown in Fig. 2. For instance, at 500 K, this second frequency occurs at 105 cm$^{-1}$ versus 58 cm$^{-1}$ for the main AFD frequency. Such a second AFD frequency has a peak that is much weaker than the one associated with the main AFD resonant frequency and is caused by alloy effects. Note that, when using the virtual crystal approximation [19] to treat PZT, only one single AFD peak therefore exists, and two dielectric peaks of $A_1$ symmetry also occur when twice the frequency of this single AFD mode is near the FE $A_1$ frequency.

[24] E. Wilson, Phys. Rev. **46**, 146 (1934).

[25] W. Low, Phys. Rev. **97**, 1664 (1955).

[26] G. M. Gale, P. Guyot-Sionnest, W. Q. Zheng, and C. Flytzanis, Phys. Rev. Lett. **54**, 823 (1985).

[27] A. Yaremko and D. Ostrovskii, J. Phys. Condens. Matter **7**, 7833 (1995).

[28] A. Yaremko, J. Mol. Struct. **511–512**, 57 (1999).

[29] Note that the present FR occurs well within the stability range of the $P4mm$ phase, which implies that phenomena that are strictly restricted to the vicinity of the ferroelectric phase transition are not fully relevant here.

[30] See Supplemental Material at http://link.aps.org/supplemental/10.1103/PhysRevLett.107.175502 for detailed analysis of the FE-AFD nonlinear coupling and experimental results of the Fermi resonance.

[31] S. Prants, J. Phys. B **21**, 397 (1988).

[32] Please see C. Ambrosch-Draxl and P. Knoll, Physica (Amsterdam) **194–196B**, 2091 (1994) and C. Ambrosch-Draxl, *Phase Separation in Cuprate Superconductors*, edited by E. Sigmund (Springer, Berlin, 1994) for the issue about the existence of the FR effect on clusters of different sizes.

[33] W. Hayes and R. Loudon, *Scattering of Light by Crystals* (Wiley, New York, 1978).

[34] J. Frantti *et al.*, Jpn. J. Appl. Phys. **38**, 5679 (1999).

[35] K. C. V. Lima *et al.*, Phys. Rev. B **63**, 184105 (2001).

[36] E. Buixaderas, I. Gregora, S. Kamba, J. Petzelt, and M. Kosec, J. Phys. Condens. Matter **20**, 345229 (2008).